Precise location of two novel linear epitopes on the receptor-binding domain surface of MERS-CoV spike protein recognized by two different monoclonal antibodies

Pan Wang [a,b], Peiyang Ding [c], Qiang Wei [b], Hongliang Liu [c], Yunchao Liu [b], Qingmei Li [b], Yunrui Xing [b], Ge Li [b], Enmin Zhou [a], Gaiping Zhang [a,b,c,d,e,*]

[a] College of Veterinary Medicine, Northwest A&F University, Yangling 712100, China
[b] Henan Provincial Key Laboratory of Animal Immunology, Henan Academy of Agricultural Sciences, Zhengzhou 450002, China
[c] School of Life Sciences, Zhengzhou University, Zhengzhou 450001, China
[d] College of Animal Science and Veterinary Medicine, Henan Agricultural University, Zhengzhou 450002, China
[e] Jiangsu Co-Innovation Center for the Prevention and Control of Important Animal Infectious Disease and Zoonose, Yangzhou University, Yangzhou, China

ARTICLE INFO

ABSTRACT

Middle East respiratory syndrome coronavirus (MERS-CoV) is a coronavirus which can cause severe human respiratory diseases with a fatality rate of almost 36%.

In this study, we report the generation, characterization and epitope mapping of several monoclonal antibodies against the spike receptor-binding domain (RBD) of MERS-CoV. Two monoclonal antibodies (4C7 and 6E8) that can react with linearized RBD have been selected for subsequent identification of RBD mAb-binding epitopes. Two distinct novel linear epitopes, ^{423}FTCSQIS^{429} and ^{546}SPLEGGGWL^{554}, were precisely located at the outermost surface of RBD by dot-blot hybridization and ELISAs. Multiple sequence alignment analysis showed that these two peptides were highly conserved. Alanine (A)-scanning mutagenesis demonstrated that residues 423F, 428I, and 429S are the crucial residues for the linear epitope ^{423}FTCSQIS^{429} while residues 548L, 550G, 553W, 554L for epitope ^{546}SPLEGGGWL^{554}. These findings may be helpful for further understanding of the function of RBD protein and the development of subsequent diagnosis and detection methods.

1. Introduction

Middle East Respiratory Syndrome (MERS) is a fatal zoonotic disease caused by Middle East Respiratory Syndrome Coronavirus (MERS-CoV), with a mortality rate as high as 35.7% [1]. Humans infected with MERS-CoV often show non-specific symptoms, such as slight fever, aversion to cold, headache, cough, dyspnea, sore throat and muscle pain, anorexia, nausea, abdominal pain, and diarrhea [2–6]. In most of the cases, lower respiratory tract infection leading to pneumonia that causes acute respiratory distress syndrome. The reasons for the pneumonia include older age, pyrexia, lymphopenia, thrombocytopenia, increment in C-reactive protein in serum ($\geq$2 mg/dl) and high viral load in sputum [7,8].

According to a report from the World Health Organization, by the end of April 2021, a total of 2574 laboratory-confirmed cases of Middle East respiratory syndrome (MERS), including 886 associated deaths (case-fatality ratio 34.4%), were reported globally. No new cases were reported during this month while one previously reported case passed away. (http://www.emro.who.int/health-topics/mers-cov/mers-outbreaks.html). MERS-CoV represents a second coronavirus that is extremely dangerous to human after SARS-CoV. It was first isolated and identified from a male patient in Saudi Arabia in 2012 [9], and was officially named MERS-CoV by the Coronavirus Research Group of the World Health Organization in 2013 [10]. The first case of MERS imported from South Korea appeared in China in 2015 [9], but it has not occurred since then [11]. Previous studies suggested that MERS-CoV originated in bat [12,13]. Evidence suggests that a dromedary camel was the source of MERS-CoV that infected a patient who had close contact with the camel's nasal secretions. Camels may act as intermediate hosts that transmit the virus from its reservoir to humans. Among dromedaries, seroprevalence field surveys have been conducted in a number of countries. To date, MERS-CoV RNA or MERS-CoV-specific antibodies have been identified in dromedaries in many countries

---

* Corresponding author at: College of Veterinary Medicine, Northwest A&F University, Yangling 712100, China.
E-mail address: zhanggaip@126.com (G. Zhang).

except Australia, Kazakhstan, and the Netherlands [14].

Genetic and phylogenetic characterization has shown that MERS-CoV belongs to lineage C of the genus of Betacoronavirus [15]. It is currently the sixth known coronavirus that can cause human diseases.

The MERS-CoV is an enveloped single-stranded positive-sense RNA virus with the genome of about 30 kb and contains at least 10 predicted open reading frames. Nine ORFS are expressed from 7 subgenomic mRNAs (sg mRNAs), which are then translated to 4 major viral structural proteins, including spike (S), envelope (E), membrane (M), and nucleocapsid (N), and several accessory proteins, 3, 4a, 4b, 5, and 8b, with origins and functions not clear. The ORF1ab genomic RNAs at the 5′-end are translated into 16 functional nonstructural proteins (nsps) that are related to viral RNA recombination and synthesis [15].

Like other coronaviruses, MERS-CoV uses its envelope spike (S) glycoprotein for interaction with a cellular receptor for entry into the target cell [16]. The S protein is composed of a N-terminal globular S1 subunit, a membrane-proximal S2 subunit and a transmembrane domain. The S1 subunit contains the determinants of host range and cellular tropism which are located in the receptor binding domain (RBD), while the S2 subunit contains mediators of membrane fusion [17–20]. RBD consists of approximately 240 amino acids and has two subunits: core subdomain and receptor binding subdomain [21–23]. It is identified that human CD26 (also known as human dipeptidyl peptidase 4, hDPP4) functions as the cellular receptor for MERS-CoV [16]. The crystal structure of MERS-CoV RBD bound to the extracellular domain of human DPP4 revealed that the RBD directly interacts with blades 4 and 5 of DPP4 propeller [24,25].

There are no approved vaccines or therapies for MERS until now. Mouse, camel, or human-derived neutralizing mAbs targeting RBD have been developed [26]. Vaccines are the most important approach against viral infections, but usually hard to develop. Neutralizing monoclonal antibodies (mAbs) have recently became a promising way to provide prophylactic and therapeutic protection of virus infections [27].

In addition, the MERS-CoV RBD contains major neutralization epitopes, induce most of the host immune responses, and could serve as the subunit vaccine against MERS-CoV infection [28–31]. Therefore, studies that focus on identification of epitopes of MERS-CoV RBD, especially the conserved epitopes, would be of great importance for vaccine and diagnostic tools development.

In this study, we immunized the BALB/c mice with RBD protein and prepared five mouse monoclonal antibodies, two of which (4C7 and 6E8)can recognize the linearized RBD protein. Among the five mAbs, only 12G9 have neutralization activity by using MERS-CoV pseudotyped virus-based assay, while the other four (4C7,6E8,7D11,5F8) did not have. Linear epitopes were further identified by scanning with truncated proteins and overlapping peptides. Consequently, two dominant epitopes, namely ^{423}FTCSQIS^{429} and ^{546}SPLEGGGWL^{554}, were located precisely. Alanine-scanning mutagenesis revealed that residues 423F, 428I, 429S, and 548L, 549E,550G, 553W, 554L were the core binding sites involved in antibody recognition. The B cell linear epitopes information obtained in this study might be valuable for further research of the function of RBD protein and in different aspects of the diagnosis of MERS-CoV.

2. Materials and methods

2.1. Cell, plasmid and virus

Human embryonic kidney 293F cells (HEK 293F) were obtained from ATCC (Manassas, VA, USA). The *Spodoptera frugiperda*. 21 cells (sf21) were obtained from Invitrogen. SP2/0 myeloma cells were kept by the Henan Provincial Key Laboratory of Animal Immunology (Zhengzhou, China). HEK 293F cells were cultured in SMM 293-TII medium (Sino biological, Beijing, China), and SP2/0 cells were cultured in Dulbecco's modified Eagle's medium (DMEM; Solarbio, Beijing, China) supplemented with 10% (v/v) fetal bovine serum (FBS, Gibco, USA). The sf21

cells were cultured in Sf-900 II SFM (serum free Insect Cell Culture Medium, Invitrogen, USA) DH10Bac and JM109 were purchased from Weidi Biotechnology Co. Ltd. (Shanghai, China). The eukaryotic expression vectors pFastBac1 (Invirogen, USA) and pcDNA3.1 were used to express the MERS-CoV RBD and the RBD truncations, respectively.

2.2. Expression of MERS-CoV RBD protein

The complete coding sequence (CDS) of MERS-CoV RBD gene (GenBank accession AFS88936.1, 367-606aa) was synthesized and subcloned into the pcDNA3.1 vector. The recombinant plasmid was transfected into the HEK 293F cells for the expression of S-RBD with a C-His tag. The resultant protein was named MRBD-His. For the expression of RBD using baculovirus expression system, the coding sequence of rabbit IgG Fc (rFc) was inserted at the C-terminus of RBD. The RBD-rFc gene was then subcloned into the pFastBac1 vector. Recombinant baculovirus was generated using the Bac-to-Bac system and sf21 cells were infected for large-scale protein production. The recombinant protein was named MRBD-rFc. These two recombinant proteins were confirmed by western blotting using anti-his tag (HRP-Conjugated His-Tag Monoclonal Antibody, proteintech, Wuhan, Hubei, China,HRP-66005) mAb and anti-rFc antibody (Anti-Rabbit IgG Fc antibody, abcam,USA,ab190492), respectively.

2.3. Monoclonal antibodies generation and characterization

Three 6–8-week-old female BALB/c mice were subcutaneously immunized with 1 μg MRBD-His protein emulsified with Freund's complete adjuvant (SigmaAldrich, Shanghai, China). The following three subcutaneous immunization was performed with the same dosage of antigen emulsified with Freund's incomplete adjuvant (Sigma-Aldrich, Shanghai, China) at 2-week intervals. The mouse serum samples were collected and determined by the indirect enzyme-linked immunosorbent assay (ELISA) at 14 dpi, 28 dpi, 42dpi and 56 dpi. Subsequently, the mouse with the highest MRBD-specific antibody titers was given the last booster immunization with 2 μg MRBD-His protein in PBS by intraperitoneal injection at 60 dpi. Five days after the last booster immunization, the mice were sacrificed and the splenocytes were fused with SP2/0 murine myeloma cells. The fused hybridoma cells were selected from unfused myeloma and spleen cells in hypoxanthine-aminopterin-thymidine (HAT) medium and then hypoxanthine-thymidine (HT) medium. The positive hybridoma cells were screened by indirect ELISA and subcloned three times by the limiting dilution method. After subcloning, the positive hybridoma cells were injected into BALB/c mice and the ascites fluid were collected and purified by protein G column chromatography (GE Healthcare, USA) according to the manufacturer's instructions. The isotypes of these mAbs were determined using the mouse monoclonal antibody subtype identification kit (Proteintech, Wuhan, China).

2.4. Indirect ELISA method

The 96-well plates (MaxiSorp, Thermo Fisher Scientific Inc., USA) were coated with the purified MRBD-rFc (2.5 μg/ml, 100 μl/well) in carbonate–bicarbonate buffer (CBS, pH 9.6) and incubated at 37 °C for 2 h. After 5 times of washing with PBST (1× PBS with 0.05% Tween 20, pH 7.4), the plates were incubated with 5% skim milk at 37 °C for 2 h. The hybridoma clone supernatants or ascites fluid were added into the 96-well plates and incubated at 37 °C for 1 h. Then the wells were washed with PBST as before and then incubated with horseradish peroxidase (HRP)-conjugated goat anti-mouse IgG (H + L) (Abbkine, AmyJet Scientific, Wuhan, China) for 1 h, followed by 5 times of washing with PBST. The reactions were developed using 3,3′,5,5′-tetramethylbenzidine (TMB). 2 M H_2SO_4 was used to stop the reaction. The OD values of each well were measured at 450 nm using a microplate reader (Omega, Germany).

2.5. Immunofluorescence assay

The specificity of anti-MERS-CoV RBD mAbs was confirmed by IFA. HEK293T cells cultured in DMEM supplemented with 10% FBS were seeded into 6-well cell culture plates at a density of 2×10^6 cells/well and incubated for 24 h at 37 °C with 5% CO_2. When the cells in each well were 70–90% confluent, the recombinant plasmid pEGFP-C1-MRBD was transfected into the cells using Lipofectamine® 2000 (Invitrogen, Life Technologies, USA) and cultured at 37 °C for 24 h. Subsequently, the plates were fixed with 4% paraformaldehyde for 15 min at room temperature (RT). Then the plates were washed with PBST and incubated with 5% skim milk at 37 °C for 2 h. After being washed for 5 times with PBST, the plates were incubated with anti-MERS-CoV RBD mAbs at RT for 1 h. The mAb against SARS-CoV2 RBD was used as a negative control. The plates were then washed for 3 times with PBST and incubated with goat anti-mouse IgG H + L-Alexa Fluor® 647 (Abcam, Shanghai, China) for 30 min at 37 °C. Cells were simultaneously stained by 4′,6-diamidino-2-phenylindole (DAPI, Solarbio, Beijing, China). After the final wash, the fluorescence signals were visualized by fluorescence microscopy (ZEISS, Jena, Germany).

2.6. MERS-CoV pseudotyped virus based neutralization assay

The methods of this test are basically following the published protocols of Nie. et al. [32]. The MERS-CoV S protein full-length gene (GenBank accession: JX869059.2) was synthesized by Sangon Biotech (Shanghai, China). MERS-CoV pseudotyped viruses are prepared and cryopreserved at −80 °C. The MERS-CoV pseudotyped virus neutralization assay begins with serial dilutions of the samples (the five mAbs) to be tested in 96-well plate, which are then mixed with a certain amount (1×10^4 TCID50/ml) of pseudotyped virus. Then the target cells Huh-7 (2×10^5/ml) are incubated for 24 h, and the amount of pseudotyped virus entering the target cells is calculated by detecting the expression of luciferase. The cell control (CC) with only cells and the virus control (VC) with virus and cells are set up in each plate. When the raw data (Supplementary file) for control and samples are exported from the luminometer, the infection inhibition rates of each dilution of the five mAbs are calculated according to the average RLU values as follows: inhibition rate = [1 − (average RLU of sample − average RLU of CC) / (average RLU of VC − average RLU of CC)] × 100%. RLU, relative light unit; CC:cell control; VC: virus control.

2.7. Expression of MERS-CoV RBD truncated constructs

To identify the linear epitope of MERS-CoV RBD, the truncated RBD constructs were designed as a series of overlapping fragments such that each fragment overlapped with the next fragment in a 5- or 8-amino-acid overlap zone (Fig. 3A and B). The primers used to clone each truncated construct are shown in Table 1. The cDNAs encoding truncated MERS-CoV RBD constructs were inserted into the pFuse-hIgG1-FC2 vector (Invitrogen, USA) using restriction enzyme sites *Eco*RI and *Nco*I. After transient expression in HEK-293T cells for 48 h, truncated MERS-CoV RBD proteins were enriched by using HiTrap Protein G HP column (GE Healthcare, USA). Target proteins were eluted with 0.1 M glycine-HCl buffer (pH 2.7) and neutralized using 1 M Tris-HCl (pH 9.0).

2.8. Identification of the linear epitopes

Dot immunoblotting assay was employed to determine the epitopes recognized by mAbs. hIgG1-Fc (human)-tagged MERS-CoV RBD truncated proteins or synthetic peptides were spotted onto nitrocellulose (NC) membranes (Pierce, USA). After being dried, the membranes were blocked with 5% skim milk at 4 °C overnight. After six times of washing with PBST, the membranes were incubated with 1:5000 diluted ascites fluid or mouse anti-human IgG Fc-tag monoclonal [JDC-10] antibody (Abcam, China, ab99757) at 37 °C for 1 h. HRP-conjugated goat anti-mouse IgG antibody was used as the secondary antibody, and the results were tested by incubating with NcmECL Ultra ECL (Enhanced Chemiluminescent, NCM BIO.CTD, China) reagent. Meanwhile, the corresponding indirect ELISA experiments were carried out to evaluate the reactivity of proteins or peptides with monoclonal antibodies. The procedure was the same as described in Section 2.4.

2.9. Alanine-scanning mutagenesis

Residues of peptide [423]FTCSQIS[429] and [546]SPLEGGGWL[554] were substituted one by one with alanine (A) as shown in Table 6. Mutant peptides were firstly coupled with BSA as described above, and then served as antigens. Two synthetic peptides, N1-4 and C2-1, which were renamed P1 ([412]TKLLSLFSVNDFTCSQISPAAI[433]) and P2 ([542]RKQLSPLEGGGWLVASGSTV[561]) respectively. MRBD-rFc was used as the positive control. BSA was used as the negative control. Mutant peptides were analyzed by using 6E8 or 4C7 as the primary antibody.
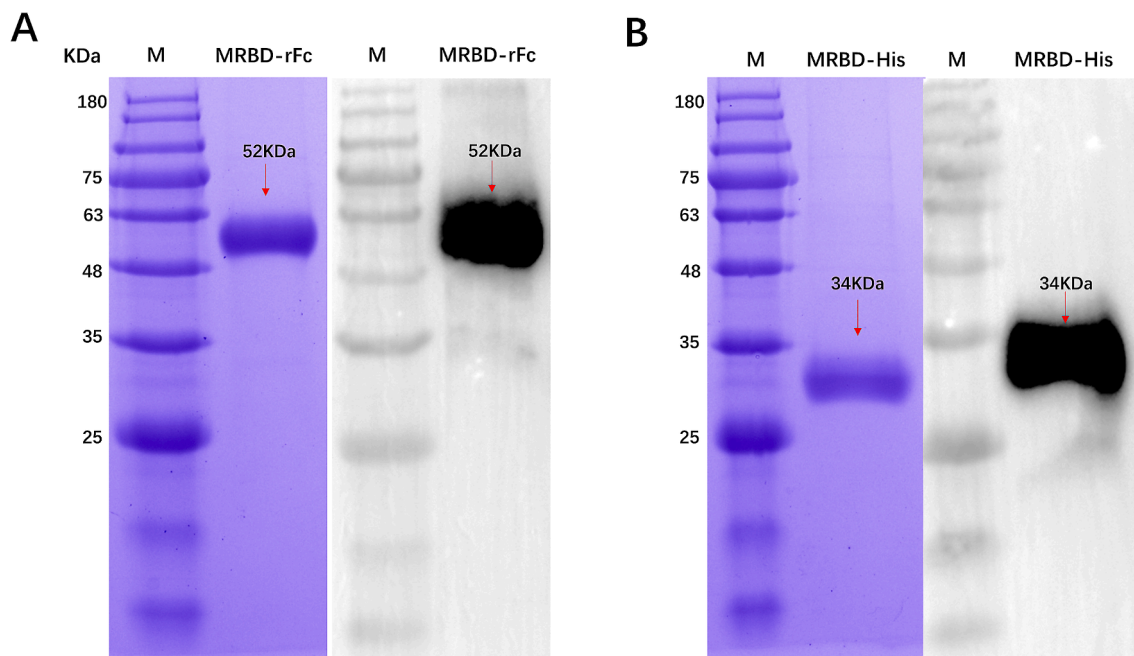
2.10. Analysis of biological information

The spatial distribution and structural property of the identified epitope was analyzed by mapping epitope on the structure of the RBD of MERS-CoV spike (PDB ID: 4kqz) using PyMOL Molecular Graphics System (Version 2.3.0, Schrödinger, LLC) and DNASTAR Protean software (DNASTARInc., USA), respectively. Epitope conservation was identified by multiple sequence alignment of RBD protein from different MERS-CoV reference strains MEGA 7.0.

3. Results

3.1. Preparation of the two recombinant MERS-CoV RBD proteins

As Section 2.2 described, The MRBD-rFc protein with C-terminal rabbit Fc tag was expressed in sf21 insect cells and enriched by using HiTrap Protein G HP column (GE Healthcare, USA). Target proteins were eluted with 0.1 M glycine-HCl buffer (pH 2.7) and neutralized using 1 M Tris-HCl (pH 9.0) as the manufacturer's instruction (Fig. 1A, left),while the MRBD-His protein with N-terminal signal peptide and C-terminal His tag was expressed in HEK 293F cells. The supernatant with soluble target protein was purified by GE HisTrap excel affinity chromatography columns according to the manufacturer's instruction (Fig. 1B, left).

Meanwhile, The western-blot assay showed that purified MRBD-rFc protein could be recognized by Anti-Rabbit IgG Fc antibody (Fig. 1A, right) with a molecular weight of approximately 52 kDa. The MRBD-His protein could be recognized by His-Tag Monoclonal Antibody (Fig. 1B, right), and it had a molecular weight of approximately 34 kDa.

Table 1
Primers used for construction of MERS-CoV RBD truncations[a].

Name	Sequence (5′-3′)	Residues sites
N-F	ccg**gaattc**ggaggctaaacctagc	367-490aa
N-R	catg**ccatgg**cggttgtcagattatgg	
N1-F	ccg**gaattc**ggaggctaaacctagc	367-433aa
N1-R	catg**ccatgg**cgatggcggctggagag	
N2-F	ccg**gaattc**gagccagatctctcca	426-490aa
N2-R	catg**ccatgg**cggttgtcagattatgg	
C-F	ccg**gaattc**gacagtgccccataatct	483-606aa
C-R	catg**ccatgg**cgtactccacgcaat	
C1-F	ccg**gaattc**gacagtgccccataa	483-549aa
C1-R	catg**ccatgg**cctccagagggctcag	
C2-F	ccg**gaattc**gagaaaacagctgagcc	542-606aa
C2-R	catg**ccatgg**cgtactccacgcaattg	

[a] The underlined letters represented restriction enzyme sites.

Fig. 1. Preparation and characterization of the two recombinant MERS-CoV RBD proteins. (A) SDS-PAGE and western blot results of the purified MRBD-rFc protein. MRBD-rFc protein comprises 464 amino acids and has a predicted molecular mass of approximately 52 kDa. (B) SDS-PAGE and western blot results of the purified MRBD-His protein. MRBD-His protein consists of 251 amino acids and predicts a molecular mass of 27.7 kDa. As a result of glycosylation, it migrates as an approximately 34 kDa band in SDS-PAGE under reducing conditions.

3.2. MRBD-His immunization and antibody responses in mice

BALB/c mice were immunized with MRBD-His antigen at 14-day intervals. Mice serum samples were collected and detected by ELISA (Fig. 2A and B). As shown in Fig. 2C, the serum antibody titers from MRBD-His immunized group reached 1:4096,000, which were significantly higher than PBS group, indicating that the MRBD-His protein induced intensive antibody response in mice.

3.3. Screening and characterization of anti-RBD mAbs

The mouse with highest antibody titer in Fig. 1C was selected to generate mAbs against MERS-CoV RBD. MRBD-rFc-based ELISA was performed to screen for the positive hybridoma cells. Through several rounds of subcloning, five hybridoma cell lines secreting desired mAbs were obtained. We named them 4C7, 6E8, 7D11, 5F8, 12G9, separately. The subtype of the five mAbs was all IgG1, and the light chain of all mAbs was Kappa (Table 2). Results from western blotting showed that 4C7 and 6E8 reacted with the denatured MERS-CoV RBD, suggesting that these two mAbs recognize the linear epitopes (Fig. 3A). Meanwhile, the remaining three mAbs supposed to bind with conformational epitopes, which did not recognize the denatured MERS-CoV RBD protein (data not shown). The results of ELISA demonstrated that all the five mAbs can recognize MRBD-rFc (Fig. 3B). The results of IFA further confirmed that all the five mAbs could specifically bind to MERS-CoV RBD (Fig. 3C). As shown in Fig. 3C, the red fluorescence excited by Alexa Fluor® 647 mainly appeared at the extranuclear area of the HEK293T cells which were transfected with the plasmid pEGFP-C1-MRBD (Table 3).

3.4. Neutralization assay of anti-RBD mAbs

Following the methods in Section 2.6, we used the formula described above to calculate the inhibition rate of the samples. In this test, the average RLU of CC is 18.1667, average RLU of VC is 24,623.5. The initial dilution of the mAb samples was 1:30 and the final dilution of was 1:7290 (3 fold dilution). As a result, mAb 12G9 have an approximately
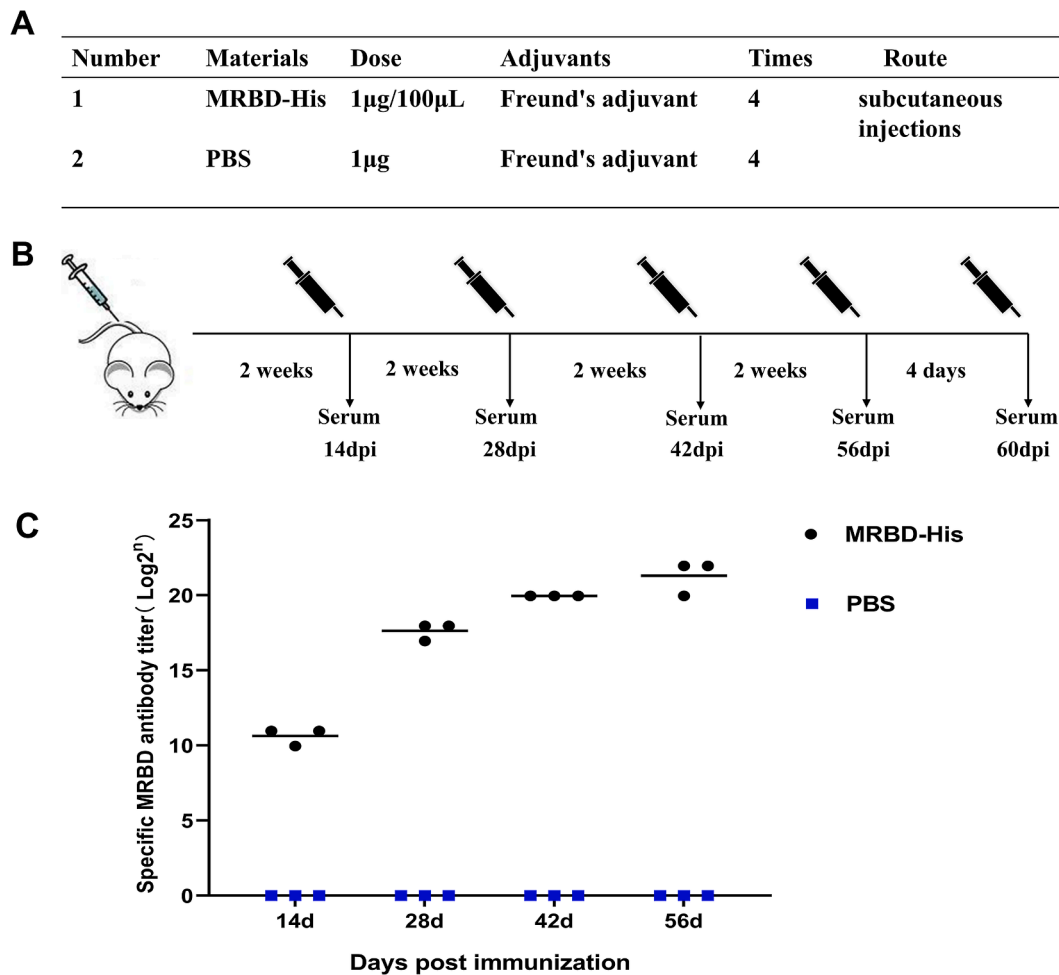
50% inhibition rate at the dilution of 1:810, while the other four mAbs cannot inhibit the pseudotyped virus entry the target cell even at the initial dilution (Fig. 4).

3.5. Epitope mapping of anti-MERS-CoV RBD mAbs

On the basis of the above results, 4C7 and 6E8 were chosen for further mapping of specific linear B-cell epitopes. A total of six truncated MERS-CoV RBD overlapping fragments were constructed and expressed in HEK-293 T cells (Fig. 5A). Dot blot results showed that truncated fragments N and N1 could be recognized by mAb 6E8 while C and C2 could be recognized by mAb 4C7 (Fig. 5B). Eight peptides based on the amino acid sequence of N1 and C2 namely N1-1, N1-2, N1-3, N1-4, C2-1, C2-2, C2-3, C2-4, were designed and synthesized. Dot blot and ELISA results showed that only N1-4 and C2-1 could be recognized by the mAb 6E8 and 4C7, respectively (Fig. 5C). These two synthetic peptides, N1-4 and C2-1, were renamed P1 ([412]TKLLSLFSVNDFTCSQISPAAI[433]) and P2 ([542]RKQLSPLEGGGWLVASGSTV[561]), respectively. In order to determine the precise recognition epitopes, peptide P1 and P2 were further truncated and characterized by removing the amino acids one by one from the N-terminus and C-terminus until the accurate position of the epitope was determined (Tables 4, 5). As shown in Fig. 6A and C, the mAb 6E8 could well recognize the N-truncated peptides until the 423F residue was removed, while the mAb could recognize the C-truncated peptides until the 429S residue was deleted (Fig. 6A). Thus, the minimal motif of P1 recognized by the mAb 6E8 was [423]FTCSQIS[429]. As shown in Fig. 6B and D, the mAb 4C7 could recognize the N-truncated peptides of P2 until the 546S residue was removed. Meanwhile, mAb 4C7 could not react to C-truncated peptides of P2 when 554L was substituted. These results suggest that the minimal motif of P2 recognized by the mAb 4C7 was [546]SPLEGGGWL[554].

3.6. Core binding sites of the linear epitopes for the mAbs 6E8 and 4C7

In order to define the crucial residues involved in peptide binding by mAbs 6E8 and 4C7, each residue of the two identified linear epitopes ([423]FTCSQIS[429] and [546]SPLEGGGWL[554]) was sequentially substituted by

A

Number	Materials	Dose	Adjuvants	Times	Route
1	MRBD-His	1μg/100μL	Freund's adjuvant	4	subcutaneous injections
2	PBS	1μg	Freund's adjuvant	4	

B

C

Fig. 2. Immunization strategies and antibody responses in mice. (A) Details regarding the antigen dosage, immunization frequency and routes. (B) Schematic representation of immunization and sampling. Immunizations were performed three times in total at two-week intervals, and blood samples were collected before each immunization. (C) Titers of serum samples were detected by ELISA.

Table 2
Characteristics of mAbs.[a]

mAbs	Epitope type	Subclass/light chain	Hybridoma supernatants titers	Ascitic fluid titers	Neutralization titers
4C7	Linear	IgG1, Kappa	1:8000	1:16384,000	NC
6E8	Linear	IgG1, Kappa	1:16,000	1:8192,000	NC
7D11	Conformational	IgG1, Kappa	1:4000	1:4096,000	NC
5F8	Conformational	IgG1, Kappa	1:8000	1:8192,000	NC
12G9	Conformational	IgG1, Kappa	1:4000	1:8192,000	1:810

[a] A total of 5 mAbs was listed. Neutralization titers obtained by MERS-CoV pseudotyped virus neutralization assay. NC, mAbs did not have a neutralization activity.

alanine (Table 6). As shown in Fig. 7A, the alanine-scanning mutagenesis of epitope ^{423}FTCSQIS^{429} revealed that no binding of mAbs was observed to peptides with alanine substitutions of 423F, 428I, and 429S, implying that residues 423F, 428I, and 429S were the crucial residues for the linear epitope ^{423}FTCSQIS^{429}. Meanwhile, for epitope ^{546}SPLEGGGWL^{554}, the substitution of residues 548L, 549E, 550G, 553W, 554L with alanine resulted in the loss of antigenicity (Fig. 7B), indicating that the five residues were the core binding sites of epitope ^{546}SPLEGGGWL^{554}.

3.7. Spatial structures and position of the linear epitopes

Based on the structure of the receptor binding domain (RBD) of MERS-CoV spike protein (PDB: 4KQZ), the location of the two linear epitopes were defined. As shown in Fig. 8A, the epitope ^{423}FTCSQIS^{429}

was located on β sheet and loop in secondary structure. The epitope ^{546}SPLEGGGWL^{554} was partly located on β sheet while the rest of the sequence located on α- helix and loop in secondary structure (Fig. 8A). Besides, both two epitopes were exposed on the MERS CoV RBD surface (Fig. 8B). Moreover, both epitopes showed high antigenic index but weak hydrophilicity in the analysis of the secondary structure prediction (Fig. 8C).

3.8. The conservation of the identified linear epitope among different MERS CoV reference strains

As shown in Fig. 9A, RBD protein sequence from MERS CoV China strain (GenBank accession AFS88936.1) used in this work, and 49 representative MERS CoV strains from different countries and areas were selected for phylogenetic analysis by MEGA 7.0. Multiple sequence
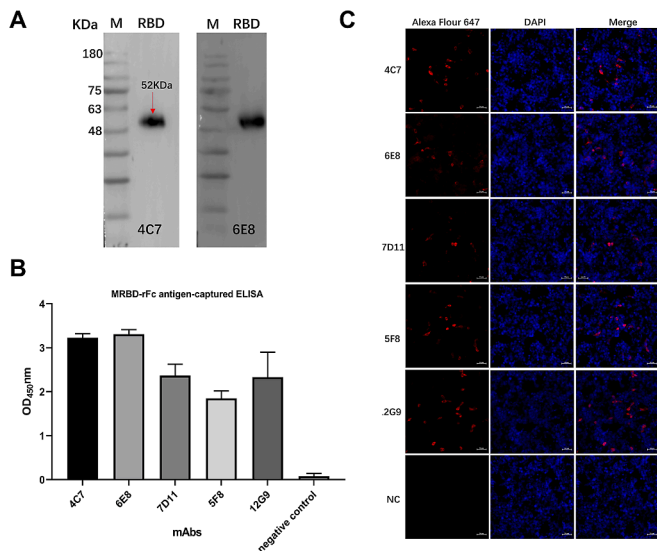
Fig. 3. Characterization of anti- MERS CoV RBD mAbs. (A) Analysis of the reactivity of mAbs with denaturedprotein MRBD-rFc. The MRBD-rFc was expressed by baculovirus expression system with a C-rFc (rabbit IgG Fc) tag. The molecular weight of MRBD-rFc was about 52KDa, which was consistent with the results of western blotting. (B) Binding of the mAbs with HEK293T cells transfected with plasmid pEGFP-C1-MRBD. MAbs specific to MRBD (red). Nuclei (blue). The HEK293T cells transfected with pEGFP-C1 plasmid were taken as the negative control (NC). Scale bars, 50 μm. (C) ELISA results for binding characteristics of mAbs with the purified MRBD-rFc. Hybridoma clone supernatants were at dilutions of 1:2000, and SP2/0 cell culture supernatants were used as the negative control. The data has been tested in three independent replicates, and the OD_{450} values were presented as means with error bars. (For interpretation of the references to colour in this figure legend, the reader is referred to the web version of this article.)

Table 3

Subsequent amino acid sequence synthesis of peptides N1 and C2.

Synthetic peptide name	Peptide sequences
N1-1	EAKPSGSVVEQAEGVECDFS
N1-2	ECDFSPLLSGTPPQVYNFKR
N1-3	YNFKRLVFTNCNYNLTKLLS
N1-4 (P1)	TKLLSLFSVNDFTCSQISPAAI
C2-1 (P2)	RKQLSPLEGGGWLVASGSTV
C2-2	SGSTVAMTEQLQMGFGITVQ
C2-3	GITVQYGTDTNSVCPKLEFA
C2-4	KLEFANDTKIASQLGNCVEY
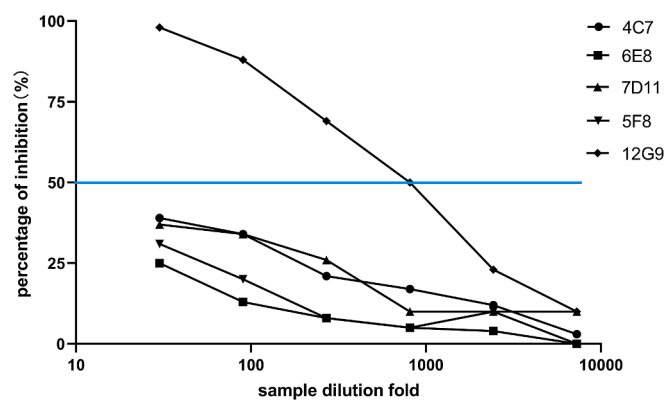
Fig. 4. The MERS-CoV pseudotyped virus infection inhibition rates of the five mAbs. Each point corresponding to the line chart represents the average RLU value (2 independent replicates) of each mAb in serial dilutions.
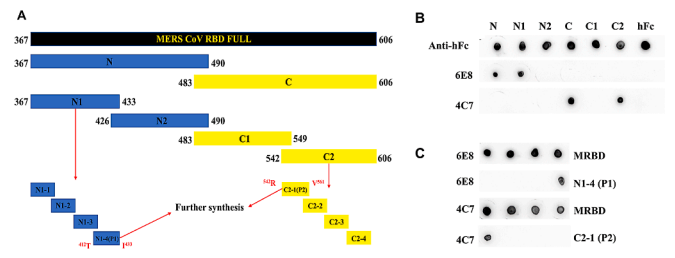
Fig. 5. Identification of the B-cell epitopes. (A) Schematic diagram of the location and length of the truncated MERS-CoV RBD protein. Amino acid regions of the various truncated fragments with 8-or 5-(for N1, C2 truncated fragments) amino acids overlap. Truncated polypeptides N, N1, N2, C, C1, and C2 were cloned into pFuse-hIgG1-FC2 vector, and expressed as fusion proteins with a hFc tag Peptides N1-1, N1-2, N1-3, N1-4, C2-1, C2-2, C2-3, C2-4, were synthesized by GL Biochem (Shanghai, China).(B) (C) Binding results of mAbs with the truncated MERS-CoV RBD protein and synthesized peptides were obtained using dot immunoblotting assay.

Table 4

N- terminal and C-terminal truncation of peptide P1.

Name	N-terminal truncation	Name	C-terminal truncation
P1-N1	KLLSLFSVNDFTCSQISPAAI	P1-C1	TKLLSLFSVNDFTCSQISPAA
P1-N2	LLSLFSVNDFTCSQISPAAI	P1-C2	TKLLSLFSVNDFTCSQISPA
P1-N3	LSLFSVNDFTCSQISPAAI	P1-C3	TKLLSLFSVNDFTCSQISP
P1-N4	SLFSVNDFTCSQISPAAI	P1-C4	TKLLSLFSVNDFTCSQIS[a]
P1-N5	LFSVNDFTCSQISPAAI	P1-C5	TKLLSLFSVNDFTCSQI
P1-N6	FSVNDFTCSQISPAAI	P1-C6	TKLLSLFSVNDFTCSQ
P1-N7	SVNDFTCSQISPAAI	P1-C7	TKLLSLFSVNDFTCS
P1-N8	VNDFTCSQISPAAI	P1-C8	TKLLSLFSVNDFTC
P1-N9	NDFTCSQISPAAI	P1-C9	CTKLLSLFSVNDFT[b]
P1-N10	DFTCSQISPAAI	P1-C10	CTKLLSLFSVND
P1-N11	FTCSQISPAAI[a]	P1-C11	CTKLLSLFSVN
P1-N12	TCSQISPAAI	P1-C12	CTKLLSLFSV

[a] The minimal residues of N- terminal and C- terminal truncation.
[b] The additional Cysteine is added to improve the coupling efficiency of BSA and peptides.

Table 5

N- terminal and C-terminal truncation of peptide P2.

Name	N- terminal truncation	Name	C- terminal truncation
P2-N1	CKQLSPLEGGGWLVASGSTV[b]	P2-C1	CRKQLSPLEGGGWLVASGST
P2-N2	CQLSPLEGGGWLVASGSTV	P2-C2	CRKQLSPLEGGGWLVASGS
P2-N3	CLSPLEGGGWLVASGSTV	P2-C3	CRKQLSPLEGGGWLVASG
P2-N4	CSPLEGGGWLVASGSTV[a]	P2-C4	CRKQLSPLEGGGWLVAS
P2-N5	CPLEGGGWLVASGSTV	P2-C5	CRKQLSPLEGGGWLVA
P2-N6	CLEGGGWLVASGSTV	P2-C6	CRKQLSPLEGGGWLV
P2-N7	CEGGGWLVASGSTV	P2-C7	CRKQLSPLEGGGWL[a]
P2-N8	CGGGWLVASGSTV	P2-C8	CRKQLSPLEGGGW
P2-N9	CGGWLVASGSTV	P2-C9	CRKQLSPLEGGG
P2-N10	CGWLVASGSTV	P2-C10	CRKQLSPLEGG
P2-N11	CWLVASGSTV	P2-C11	CRKQLSPLEG
P2-N12	CLVASGSTV	P2-C12	CRKQLSPLE

[a] The minimal residues of N- terminal and C- terminal truncation.
[b] The additional Cysteine is added to improve the coupling efficiency of BSA and peptides.
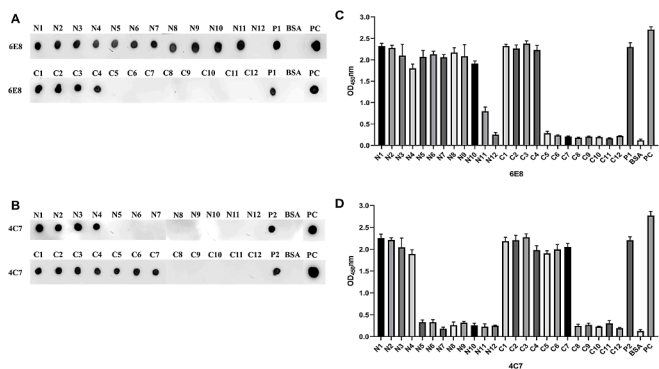
Fig. 6. Mapping of the minimum mAb recognition sequences of P1 and P2. (A–B) Binding results of mAbs with the N-terminal and C-terminal truncations of peptide P1 (A) and P2 (B) were obtained using dot immunoblotting. MRBD-rFc was used as the positive control. BSA protein was taken as negative control. (C–D) ELISA results for binding characteristics of mAb 6E8 (C) and 4C7 (D) with N-terminal and C-terminal truncations of peptide P1 and P2. The data has been tested in three independent replicates, and the OD_{450} values were presented as means and SD with error bars.

Table 6
Alanine-scanning mutagenesis of the minimal motifs of peptides ^{423}FTCSQIS^{429} and ^{546}SPLEGGGWL^{554}.[a]

Substitution	Peptide sequences	Substitution	Peptide sequences
423F	ATCSQIS	546S	BSA-CAPLEGGGWL
424T	FACSQIS	547P	BSA-CSALEGGGWL
425C	BSA-CFTASQIS	548L	BSA-CSPAEGGGWL
426S	FTCAQIS	549E	BSA-CSPLAGGGWL
427Q	FTCSAIS	550G	BSA-CSPLEAGGWL
428I	FTCSQAS	551G	BSA-CSPLEGAGWL
429S	FTCSQIA	552G	BSA-CSPLEGGAWL
		553W	BSA-CSPLEGGGAL
		554L	BSA-CSPLEGGGWA

[a] The additional Cysteine is added to improve the coupling efficiency of BSA and peptides.

alignment analysis was performed to evaluate the conservation of the identified epitopes among different MERS CoV strains. As shown in Fig. 9B, alignment of amino acid sequences of RBD protein from

different MERS CoV strains revealed that both of the two epitopes were highly conserved. For epitope ^{423}FTCSQIS^{429}, only 424 T was mutated to 424I in strain ASU90164.1 (camel/UAE/2015). For epitope ^{546}SPLEGGGWL^{554}, 553W was mutated to 553R in strain AWU59321.1 (human/Saudi Arabia/2016). Besides, we also did the phylogenetic analysis from random reference sequences of all the seven coronaviruses that can infect human (Supplementary Fig. 1). The phylogenetic tree shows that SARS-CoV-2 is closer to the SARS-related coronavirus sequence, and they are located at the bottom of the tree, indicating that SARS-CoV-2 were highly homologous to SARS-related coronavirus sequence. The MERS-CoV sequences are not directly connected to the SARS-CoV-2. Compare to these lethal coronaviruses, human coronavirus (HCoV)-229E, HCoV-NL63, HCoV-OC43, or HCoV-HKU1 cause only the common cold [33]. And they are not directly connected to MERS-CoV.

4. Discussion

Corona viruses are enveloped viruses, which are further divided into four different subtypes, alpha-, beta-, gamma-, and delta-CoV [34,35]. So far, seven CoVs are confirmed can cause human diseases [36,37]. Three of beta-CoVs, SARS-CoV, MERS-CoV, and SARS-CoV-2 are life-threatening [38]. Therefore, since the discovery of MERS-CoV in 2012, MERS-CoV has attracted great attention in biomedical research [9,39].

Anti-MERS-CoV mAbs from immunized mice have isolated from several research groups [40], most reported MERS-CoV mAbs with neutralizing activities are RBD specific [41]. Generally, neutralizing mAbs targeting RBD are more potent than those targeting other regions of S protein [42]. The reported mouse neutralizing mAbs including Mersmab1, 4C2 and 2E6 were all bound to the RBD of MERS-CoV through recognizing conformational epitopes [26]. MERS-CoV S protein trimer frequently performs conformational changes, switching between a lying down and a standing up conformation, which represent receptor-inaccessible and receptor-accessible conformation [43]. When neutralizing antibodies bind to RBD, they can cause conformational change in S protein, similar to receptor–virus interaction [44]. Yang et al. identified the first linear neutralizing epitope located outside of the RBD in the S protein of MERS-CoV [45]. So far, linear neutralizing epitopes located inside the RBD have not been reported. Similarly, in SARS-CoV-2 RBD, little neutralization activity is observed for the linear-epitope-elicited antibodies [46].

To sum up, study focus on the functions of conserved epitopes of RBD
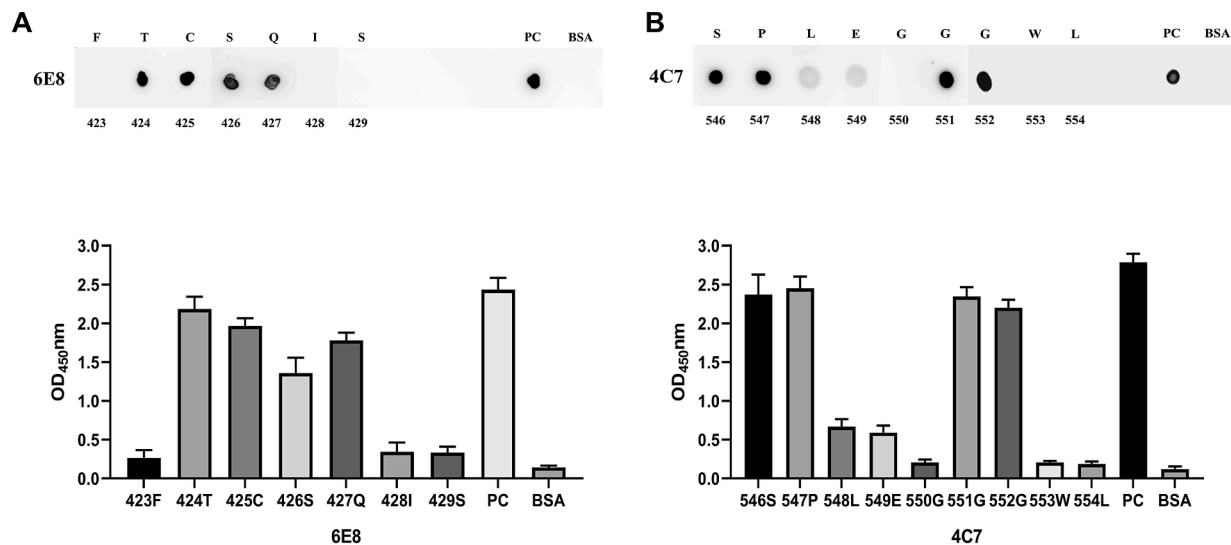
Fig. 7. Identification of the critical amino acid residues in the dominant epitope. (A–B) Binding characteristics of 6E8 (A) and 4C7 (B) with peptide mutants by ELISA and dot immunoblotting assay. MRBD-rFc was used as the positive control. BSA protein was taken as negative control. The ELISA data has been tested in three independent replicates, and the OD_{450} values were presented as means and SD with error bars.
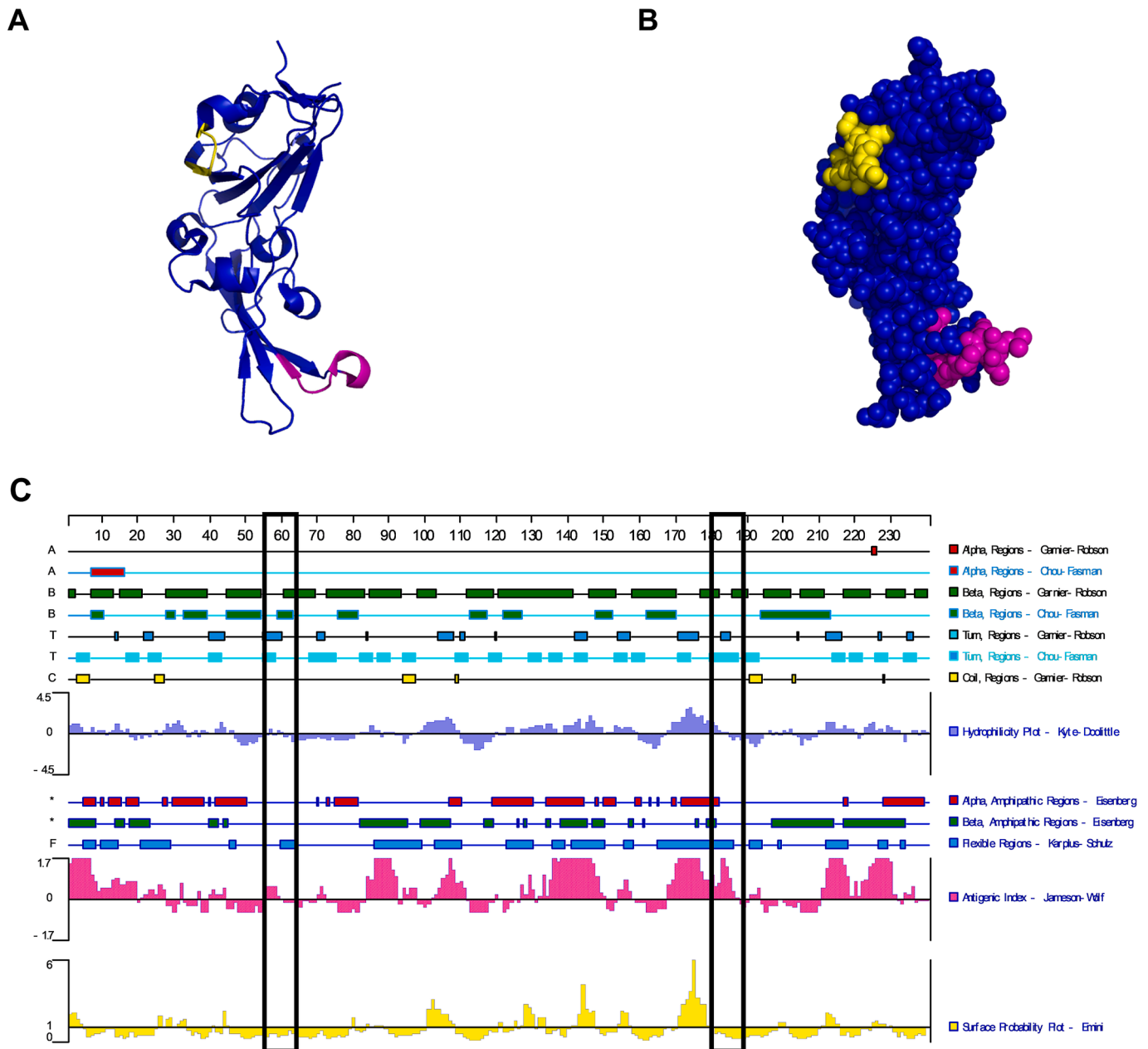
Fig. 8. Spatial localization of the core epitope. (A) Secondary structural analysis of the core epitope on the MERS-CoV monomer skeleton. (B) Spatial distributions of the core epitope in MERS-CoV RBD with a solid surface. (C) Secondary structural prediction of the RBD. epitope [423]FTCSQIS[429] and [546]SPLEGGGWL[554] was indicated in black box.

seems reasonable and promising. Moreover, the dominant epitope of the RBD protein has a greater potential use for early diagnostics than the others.

B-cell epitopes are divided into linear or conformational. According to the former studies, 10% of B cell-recognizing epitopes are linear epitopes, this is due to most of the B-cells epitopes have conformational changes in three dimensional structure, the antigen internalizing process and antigen recognizing ability [47–49].

Precise location of B-cell epitopes is crucial for the development of epitope-based diagnostic methods, vaccines, and therapeutic antibodies. Structural and functional methods are oftenly used. Although structural method like X-ray crystallography can also precisely locate the epitope position, its widespread use limited by time consuming and huge cost [50].

Consequently, the mapping of conformational epitopes is complicated and usually requires other ways to complete, such as

computational tools and phage display techniques. These methods are much more difficult than traditional linear epitope identification methods [51,52]. Functional methods are used to detect the binding efficiency of antibody with protein fragments, synthetic peptides or recombinant proteins, and more convenient to conduct [50]. Thus, the linear epitopes were chosen to be further determined. Besides, for the development of epitope-based vaccines, the specificity can be enhanced by only selecting the antigenic domains of proteins exposed on the surface in order to elicit strong immune responses [53]. Precise location of B-cell epitopes was related to antigenicity, accessibility of surface, flexibility, hydrophilicity and predictions of linear epitope [54]. Thus, those surface epitopes of the RBD were chosen.

Here, we generated and characterized mAbs specific to the RBD of MERS-CoV, and provided new insight into epitope mapping of RBD. In this study, we immunized BALB/c mice with recombinant purified MERS-CoV RBD, and screened 5 hybridoma cell lines that produced anti-
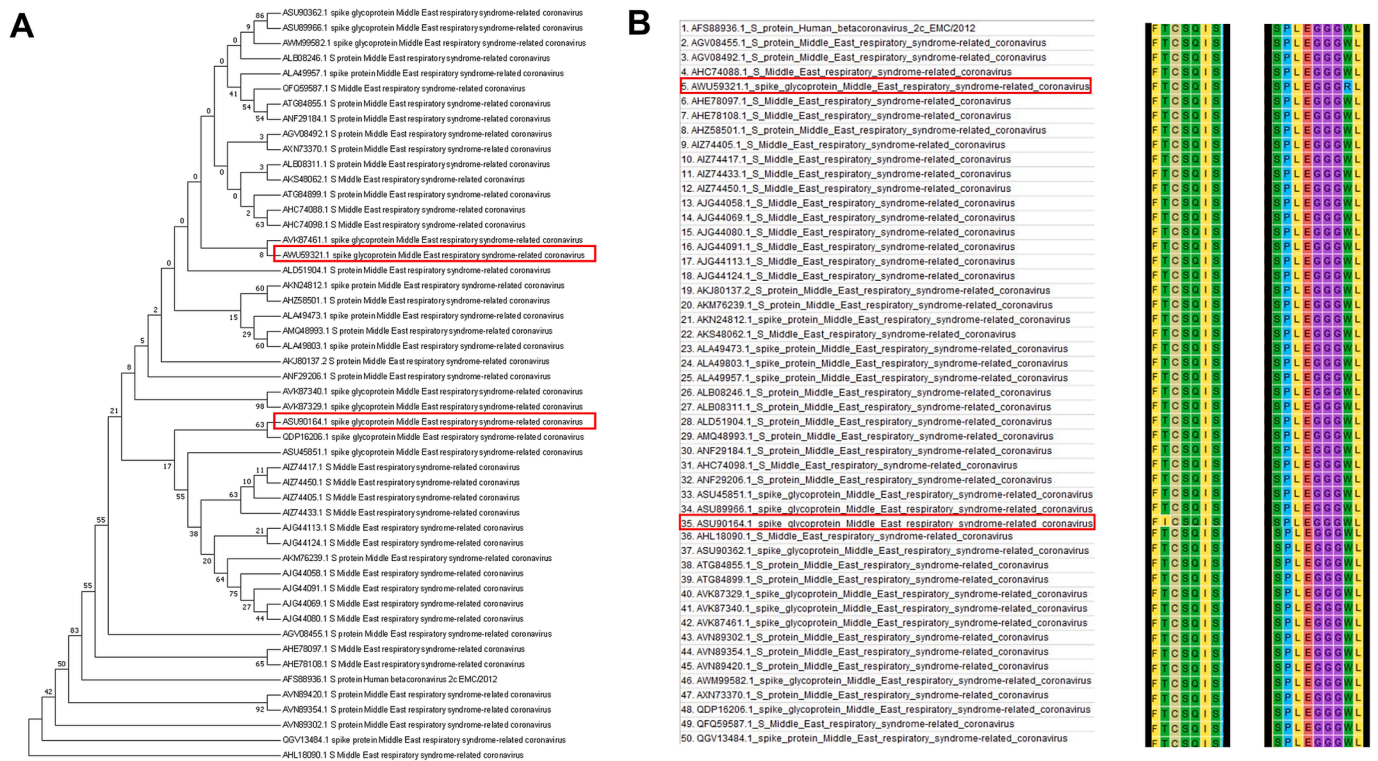
Fig. 9. The conservation of the identified epitope among different MERS-CoV reference strains. (A) Genotyping of 50 MERS-CoV strains based on S protein sequence. The phylogenetic tree was constructed using the neighbor-joining method in MEGA 7.0. (B) Alignment of RBD protein sequence from different MERS-CoV strains. Mutations in 424T and 553W showed in different colors.

MERS-CoV RBD monoclonal antibodies. Two of the mAbs (4C7 and 6E8) recognize denatured RBD protein in western blotting assay, while three other mAbs (7D11, 5F8, 12G9) did not react with the denatured RBD protein, so we speculated that they recognize the conformational epitopes. (Fig. 3). The result of pseudotyped virus-based neutralization assay showed that only mAb 12G9, which recognized the conformational epitopes, had the neutralization activity.

Subsequently, the linear epitopes recognized by mAbs 6E8 and 4C7 were scanned by truncated recombinant RBD protein and overlapping synthetic peptides. As shown in Figs. 5 and 6, the precise linear epitopes recognized by mAbs 6E8 and 4C7 were determined to be 423FTCSQIS429 and 546SPLEGGGWL554, respectively. Furthermore, we assessed the interaction between the epitope and the monoclonal antibody through alanine-scanning mutagenesis (Table 6). As shown in Fig. 7A, the 423F, 428I, and 429S mutants basically eliminated the reactivity between the peptide and monoclonal antibody 6E8. On the contrary, 424T, 425C, 426S, and 427Q mutants hardly affect the binding ability to monoclonal antibodies. Thus, the results shows that 423F, 428I, and 429S are the key amino acids of epitope 423FTCSQIS429. For epitope 546SPLEGGGWL554, when 548L, 549E, 550G, 553W, and 554L were mutated, the reactivity of the peptides with monoclonal antibody 4C7 was drastically reduced, and only light or blurry blots could be observed on the nitrocellulose membrane (Fig. 7B). Besides, the corresponding ELISA results showed that the OD$_{450}$ values of the five mutants were significantly lower than that of the 546S, 547P, 551G, and 552G mutants. Thus, the core amino acids of polypeptide 546SPLEGGGWL554 were 548L, 549E, 550G, 553W, and 554L. Notably, it is reported that the residue 553W was the key site of mouse neutralizing antibodies may inhibit DPP4 binding at, and potently neutralize infection of pseudotyped or live MERS-CoV [41,55].

Mabs targeting the RBD could recognize key residues that are crucial for DPP4 binding. Also, changing of one or several of these critical residues in RBD may lead to the emergence of escape mutant virus strains, in which the mAbs targeting the unmutant residues in RBD will reduce or lose neutralizing ability against the mutant strains [42].

According to the published MERS-CoV spike RBD structure (PDB:4KQZ), epitopes 423FTCSQIS429 and 546SPLEGGGWL554 are located in the flexible loop region of the secondary structure, and mainly exposed on the protein surface (Fig. 8A, B). It is suggested that epitopes 423FTCSQIS429 and 546SPLEGGGWL554 are the dominant epitopes of RBD, which are likely to play an important role in stimulating the antibody immune response. Besides, the results of secondary structural prediction represented that the antigenic index and hydrophilicity of epitope 546SPLEGGGWL554 were higher than the epitope 423FTCSQIS429 (Fig. 8C), indicating that epitope 546SPLEGGGWL554 may be a more important immunodominant epitope. Due to the linear conformation of the immunogens, 4C7 and 6E8 have high reactivity to the RBDs and peptides but are lack of neutralizing activity. The results suggest that the conformation of the RBD is crucial for the induction of neutralizing antibodies, and that non-neutralizing immunodominant epitopes are within the RBD of the MERS-CoV S protein.

An alignment of MERS-CoV RBD protein from 49 representative strains showed that most amino acids of the two identified epitopes were conserved (Fig. 9). For epitope 423FTCSQIS429, 424T in strain ASU90164.1 (camel/UAE/2015) was mutated to 424I. For epitope 546SPLEGGGWL554, 553W was mutated to 553R in strain AWU59321.1 (human/Saudi Arabia/2016). Analysis of the core binding sites of the linear epitopes revealed that 424T was not the crucial residue for the linear epitope 423FTCSQIS429. In contrast, the 553W was the core binding site of epitope 546SPLEGGGWL554. Thus, the results indicated that the diagnostic reagent based on the epitope 423FTCSQIS429 may be used to detected RBD protein of different MERS-CoV strains. Meanwhile, the diagnostic reagent based on the epitope 546SPLEGGGWL554 may be used to detected RBD of most MERS-CoV strains, except the strain AWU59321.1. The phylogenetic tree of seven human CoVs (Supplementary Fig. 1) showed that the MERS CoV sequences are relatively independent. Meanwhile, the amino acid sequence of the S protein of MERS-CoV is mostly inconsistent with SARS-CoV-2 and SARS-CoV. Therefore, we focus on the MERS-CoV in this research.

In summary, a total of five monoclonal antibodies were identified in this study, two of which could recognize linear epitopes. Epitopes [423]FTCSQIS[429] and [546]SPLEGGGWL[554] were precise located by mAbs 6E8 and 4C7, respectively. The crucial residues were further determined . The results of structural analysis showed that these two epitopes were exposed on the surface of the RBD. Multiple sequence alignment analysis showed that the epitopes were highly conserved. To precise locate the surface-exposed peptides, especially those B cell epitopes that are antigenic and conserved, rather than focus on the whole pathogen, which may be effectively and increase specificity [56].

To sum up, these findings may have some implications on the diagnosis of MERS-CoV and may be helpful for elucidating the biological properties of MERS-CoV RBD.

Ethical statement

All animal experiments were approved by the Animal Experiment Committee of Henan Academy of Agricultural Sciences with the approval number (LLSC100173). All the animals received humane care in compliance with good animal practice according to the animal ethics procedures and guidelines of the Institutional Animal Care and Use Committee (IACUC). All efforts were made to alleviate and minimize animal suffering.

CRediT authorship contribution statement

Pan Wang: Methodology, Formal analysis, Software, Writing and Editing. Gaping Zhang: Writing, Editing and Funding acquisition. Peiyang Ding, Qiang Wei, Enmin Zhou, Gaiping Zhang editing the paper. Hongliang Liu, Yunchao Liu, Qingmei Li, Yunrui Xing, Ge Li: Resources and Methodology.

Declaration of competing interest

The authors declare that they have no competing interests.

Acknowledgments

Appendix A. Supplementary data

Supplementary data to this article can be found online at https://doi.org/10.1016/j.ijbiomac.2021.11.192.

References

[1] D.S. Hui, E.I. Azhar, Y.J. Kim, Z.A. Memish, M. Oh, A. Zumla, Middle East respiratory syndrome coronavirus: risk factors and determinants of primary, household, and nosocomial transmission, Lancet Infect. Dis. S1473309918301270 (2018).

[2] Guery Benoit, Poissy Julien, Loubna el Mansouf, Clinical features and viral diagnosis of two cases of infection with Middle East respiratory syndrome coronavirus: a report of nosocomial transmission, Lancet 381 (9885) (2013) 2265–2272.

[3] K. Minal, P. Kimberly, K. Alan, D. Stephanie, L. Liu, L. Judith, P. Omar, P. Pam, R. Shawn, Y.F. Jaime, Clinical and laboratory findings of the first imported case of Middle East respiratory syndrome coronavirus to the United States, Clin.ical Infectious Diseases (11) (2014) 1511–1518.

[4] B. Annie, S. Sacha, C.R. Beck, J.S. Nguyen-Van-Tam, The roles of transportation and transportation hubs in the propagation of influenza and coronaviruses: a systematic review, J. Travel Med. (1) (2016) in press.

[5] M.S. Mohammed, H.S. Khalid, A.E. Muddathir, K. Eltahir, A.A. Khan, H.A. Algadir, W.J. Osman, N.A. Siddiqui, Effect of some plants' extracts used in sudanese folkloric medicines on carrageenan-induced inflammation, Pak. J. Pharm. Sci. 28 (1) (2015) 159–165.

[6] V.M. Corman, A.M. Albarrak, O.A. Senosi, M.M. Albarrak, F.M. Elamin, A. Malak, M. Doreen, S. Andrea, M. Benjamin, A.M. Assiri, Viral shedding and antibody response in 37 patients with Middle East respiratory syndrome coronavirus infection, Clin. Infect. Dis. 62 (4) (2016) 477–483.

[7] D.S. Hui, Z.A. Memish, A. Zumla, Severe acute respiratory syndrome vs. the Middle East respiratory syndrome, Curr. Opin. Pulm. Med. 20 (3) (2014) 233–241.

[8] A. Zumla, D.S. Hui, S. Perlman, Middle East respiratory syndrome, Lancet 386 (9997) (2015) 995–1007.

[9] A.M. Zaki, Brief report: isolation of a novel coronavirus from a man with pneumonia in Saudi Arabia (vol 367, pg 1814, 2012), N. Engl. J. Med. 369 (4) (2013) 394.

[10] R.D. Groot, S. Baker, R. Baric, C. Brown, C. Drosten, L. Enjuanes, R. Fouchier, M. Galiano, A. Gorbalenya, Z. Memish, Middle East respiratory syndrome coronavirus (MERS-CoV): announcement of the coronavirus study group, J. Virol. 87 (14) (2013) 7790–7792.

[11] D. Forni, R. Cagliani, M. Clerici, M. Sironi, Molecular evolution of human coronavirus genomes, Trends Microbiol. 25 (1) (2016) 35–48.

[12] S.J. Anthony, K. Gilardi, V.D. Menachery, T. Goldstein, B. Ssebide, R. Mbabazi, I. Navarrete-Macias, E. Liang, H. Wells, A. Hicks, Further evidence for bats as the evolutionary source of Middle East respiratory syndrome coronavirus, MBio 8 (2) (2017) e00373-17.

[13] Q. Wang, J. Qi, Y. Yuan, Y. Xuan, P. Han, Y. Wan, W. Ji, Y. Li, Y. Wu, J. Wang, Bat origins of MERS-CoV supported by bat coronavirus HKU4 usage of human receptor CD26, Cell Host Microbe 16 (3) (2014) 328–337.

[14] C. Drosten, P. Kellam, Z.A. Memish, Evidence for camel-to-human transmission of MERS coronavirus, N. Engl. J. Med. 371 (14) (2014) 1359–1360.

[15] S. van B.e. men, M. de Graaf, C. Lauber, Genomic characterization of a newly discovered coronavirus associated with acute respiratory distress syndrome in humans, mBio 3 (6) (2012).

[16] V.S. Raj, H. Mou, S.L. Smits, D.H. Dekkers, M.A. Muller, R. Dijkman, D. Muth, J. A. Demmers, A. Zaki, R.A. Fouchier, V. Thiel, C. Drosten, P.J. Rottier, A. D. Osterhaus, B.J. Bosch, B.L. Haagmans, Dipeptidyl peptidase 4 is a functional receptor for the emerging human coronavirus-EMC, Nature 495 (7440) (2013) 251–254.

[17] L. Du, Y. He, Y. Zhou, S. Liu, B.J. Zheng, S. Jiang, The spike protein of SARS-CoV–a target for vaccine and therapeutic development, Nat. Rev. Microbiol. 7 (3) (2009) 226–236.

[18] R.L. Graham, E.F. Donaldson, R.S. Baric, A decade after SARS: strategies for controlling emerging coronaviruses, Nat. Rev. Microbiol. 11 (12) (2013) 836–848.

[19] P.S. Masters, The molecular biology of coronaviruses, Adv. Virus Res. 66 (2006) 193–292.

[20] S.R. Weiss, S. Navas-Martin, Coronavirus pathogenesis and the emerging pathogen severe acute respiratory syndrome coronavirus, Microbiol. Mol. Biol. Rev. 69 (4) (2005) 635–664.

[21] Y. Chen, K.R. Rajashankar, Y. Yang, S.S. Agnihothram, F. Li, Crystal structure of the receptor-binding domain from newly emerged Middle East respiratory syndrome coronavirus, J. Virol. 87 (19) (2013).

[22] G. Lu, Y. Hu, Q. Wang, J. Qi, F. Gao, Y. Li, Y. Zhang, W. Zhang, Y. Yuan, J. Bao, B. Zhang, Y. Shi, J. Yan, G.F. Gao, Molecular basis of binding between novel human coronavirus MERS-CoV and its receptor CD26, Nature 500 (7461) (2013) 227–231.

[23] N. Wang, X. Shi, L. Jiang, S. Zhang, D. Wang, T. Pei, D. Guo, Structure of MERS-CoV spike receptor-binding domain complexed with human receptor DPP4, Cell Res. 23 (008) (2013) 986–993.

[24] G. Lu, Y. Hu, Q. Wang, J. Qi, F. Gao, Y. Li, Y. Zhang, W. Zhang, Y. Yuan, J. Bao, B. Zhang, Y. Shi, J. Yan, G.F. Gao, Molecular basis of binding between novel human coronavirus MERS-CoV and its receptor CD26, Nature 500 (7461) (2013) 227–231.

[25] N. Wang, X. Shi, L. Jiang, S. Zhang, D. Wang, P. Tong, D. Guo, L. Fu, Y. Cui, X. Liu, K.C. Arledge, Y.H. Chen, L. Zhang, X. Wang, Structure of MERS-CoV spike receptor-binding domain complexed with human receptor DPP4, Cell Res. 23 (8) (2013) 986–993.

[26] H.J. Han, J.W. Liu, H. Yu, X.J. Yu, Neutralizing monoclonal antibodies as promising therapeutics against Middle East respiratory syndrome coronavirus infection, Viruses 10 (12) (2018).

[27] Y. Jin, L. Cheng, H. Dan, D.S. Dimitrov, T. Ying, Human monoclonal antibodies as candidate therapeutics against emerging viruses, Frontiers of Medicine 11 (4) (2017) 9.

[28] L. Du, G. Zhao, Y. Yang, H. Qiu, L. Wang, Z. Kou, X. Tao, H. Yu, S. Sun, C.T. Tseng, S. Jiang, F. Li, Y. Zhou, A conformation-dependent neutralizing monoclonal antibody specifically targeting receptor-binding domain in Middle East respiratory syndrome coronavirus spike protein, J. Virol. 88 (12) (2014) 7045–7053.

[29] L. Jiang, N. Wang, T. Zuo, X. Shi, K.M. Poon, Y. Wu, F. Gao, D. Li, R. Wang, J. Guo, L. Fu, K.Y. Yuen, B.J. Zheng, X. Wang, L. Zhang, Potent neutralization of MERS-CoV by human neutralizing monoclonal antibodies to the viral spike glycoprotein, Sci. Transl. Med. 6 (234) (2014) 234ra59.

[30] T. Ying, L. Du, T.W. Ju, P. Prabakaran, C.C. Lau, L. Lu, Q. Liu, L. Wang, Y. Feng, Y. Wang, B.J. Zheng, K.Y. Yuen, S. Jiang, D.S. Dimitrov, Exceptionally potent neutralization of Middle East respiratory syndrome coronavirus by human monoclonal antibodies, J. Virol. 88 (14) (2014) 7796–7805.

[31] L. Dai, T. Zheng, K. Xu, Y. Han, L. Xu, E. Huang, Y. An, Y. Cheng, S. Li, M. Liu, M. Yang, Y. Li, H. Cheng, Y. Yuan, W. Zhang, C. Ke, G. Wong, J. Qi, C. Qin, J. Yan, G.F. Gao, A Universal Design of Betacoronavirus Vaccines against COVID-19, MERS, and SARS, Cell 182 (3) (2020) 722–733, e11.

[32] J. Nie, Q. Li, J. Wu, C. Zhao, H. Hao, H. Liu, L. Zhang, L. Nie, H. Qin, M. Wang, Q. Lu, X. Li, Q. Sun, J. Liu, C. Fan, W. Huang, Quantification of SARS-CoV-2 neutralizing antibody by a pseudotyped virus-based assay, Nat. Protoc. 15 (11) (2020) 3699–3715.

[33] L. Hoek, Human coronaviruses: what do they cause? Antiviral Ther. 12 (4 Pt B) (2007) 651–658.

[34] L. Liu, in: Fields Virology, 6th editionClinical Infectious Diseases, 4, 2014, p. 4.

[35] P. Woo, S. Lau, C. Lam, K. Lai, Y. Huang, P. Lee, G. Luk, K.C. Dyrting, K.H. Chan, K. Y. Yuen, Comparative analysis of complete genome sequences of three avian coronaviruses reveals a novel group 3c coronavirus, J. Virol. 83 (2) (2009) 908–917.

[36] G. Lu, Q. Wang, G.F. Gao, Bat-to-human: spike features determining 'host jump' of coronaviruses SARS-CoV, MERS-CoV, and beyond, Trends Microbio. 23 (8) (2015) 468–478.

[37] B.A. Wevers, V. Lia, Recently discovered human coronaviruses, Clin. Lab. Med. 29 (4) (2009) 715–724.

[38] L. Dai, T. Zheng, K. Xu, Y. Han, G.F. Gao, A universal design of betacoronavirus vaccines against COVID-19, MERS and SARS, Cell 182 (3) (2020).

[39] A. Bermingham, C. Ma, C. Brown, E. Aarons, M. Zambon, Severe respiratory illness caused by a novel coronavirus, in a patient transferred to the United Kingdom from the Middle East, September 2012, Eurosurveillance 17 (40) (2012).

[40] K.E. Pascal, C.M. Coleman, A.O. Mujica, V. Kamat, C.A. Kyratsous, Pre- and postexposure efficacy of fully human antibodies against spike protein in a novel humanized mouse model of MERS-CoV infection, Proc. Natl. Acad. Sci. 112 (28) (2015) 8738–8743.

[41] L. Wang, W. Shi, M.G. Joyce, K. Modjarrad, Y. Zhang, K. Leung, C.R. Lees, T. Zhou, H.M. Yassine, M. Kanekiyo, Evaluation of candidate vaccine approaches for MERS-CoV, Nat. Commun. 6 (2015) 7712.

[42] L. Du, Y. Yang, Y. Zhou, L. Lu, F. Li, S. Jiang, MERS-CoV spike protein: a key target for antivirals, Expert Opin. Ther. Targets 21 (2) (2017) 131.

[43] Y. Yuan, D. Cao, Y. Zhang, J. Ma, J. Qi, Q. Wang, G. Lu, Y. Wu, J. Yan, Y. Shi, Cryo-EM structures of MERS-CoV and SARS-CoV spike glycoproteins reveal the dynamic receptor binding domains, Nat. Commun. 8 (2017) 15092.

[44] K. Karthik, T.M.A. Senthilkumar, S. Udhayavel, G.D. Raj, Role of antibody-dependent enhancement (ADE) in the virulence of SARS-CoV-2 and its mitigation strategies for the development of vaccines and immunotherapies to counter COVID-19, Hum.Vaccines Immunother. (2020) 1–6.

[45] Y. Yang, Y. Deng, B. Wen, H. Wang, X. Meng, J. Lan, G.F. Gao, W. Tan, The amino acids 736–761 of the MERS-CoV spike protein induce neutralizing antibodies: implications for the development of vaccines and antiviral agents, Viral Immunol. 27 (10) (2014) 543–550.

[46] Y. Li, M.L. Ma, Q. Lei, F. Wang, W. Hong, D.Y. Lai, H. Hou, Z.W. Xu, B. Zhang, H. Chen, C. Yu, J.B. Xue, Y.X. Zheng, X.N. Wang, H.W. Jiang, H.N. Zhang, H. Qi, S. J. Guo, Y. Zhang, X. Lin, Z. Yao, J. Wu, H. Sheng, Y. Zhang, H. Wei, Z. Sun, X. Fan, S.C. Tao, Linear epitope landscape of the SARS-CoV-2 spike protein constructed from 1,051 COVID-19 patients, Cell Rep. 34 (13) (2021), 108915.

[47] Chia-Yu, Ivan-Chen Chang, Yen-Chen Cheng, Pei-Shiue, Seiu-Yu Tsai, Yu-Liang Lai, Identification of neutralizing monoclonal antibodies targeting novel conformational epitopes of the porcine epidemic diarrhoea virus spike protein, Sci. Rep. 9 (1) (2019) 2529.

[48] V.R. Mhv, Mapping epitope structure and activity: from one-dimensional prediction to four-dimensional description of antigenic specificity, Methods 9 (3) (1996) 465–472.

[49] D.J. Barlow, M.S. Edwards, J.M. Thornton, Continuous and discontinuous protein antigenic determinants, Nature 322 (6081) (1986) 747–748.

[50] L. Potoňáková, M. Bhide, L.B. Pulzova, An introduction to B-cell epitope mapping and in silico epitope prediction, J Immunol Res 2016 (1) (2016).

[51] C. Li, H. Liu, J. Li, D. Liu, R. Meng, Q. Zhang, S. Wulin, X. Bai, T. Zhang, M. Liu, A conserved epitope mapped with a monoclonal antibody against the VP3 protein of goose parvovirus by using peptide screening and phage display approaches, Plos One 11 (5) (2016), e0147361.

[52] P. Molek, T. Bratkovi, Epitope mapping of mono- and polyclonal antibodies by screening phage-displayed random peptide libraries, Acta Chim. Slov. 63 (4) (2016) 914.

[53] M.M. Ranjbar, S. Almasi, Immunoinformatic analysis of glycoprotein from bovine ephemeral fever virus, Biomed.Biotechnol.Res.J. 2 (3) (2018) 208-.

[54] T.M. Fieser, J.A. Tainer, H.M. Geysen, R.A. Houghten, R.A. Lerner, Influence of protein flexibility and peptide conformation on reactivity of monoclonal anti-peptide antibodies with a protein alpha-helix, Proc. Natl. Acad. Sci. 84 (23) (1988) 8568–8572.

[55] Y. Li, Y. Wan, P. Liu, J. Zhao, G. Lu, J. Qi, Q. Wang, X. Lu, Y. Wu, W. Liu, A humanized neutralizing antibody against MERS-CoV targeting the receptor-binding domain of the spike protein, Cell Res. 25 (11) (2015) 1237–1249.

[56] M. Qamar, S. Saleem, U.A. Ashfaq, A. Bari, S. Alqahtani, Epitope-based peptide vaccine design and target site depiction against Middle East respiratory syndrome coronavirus: an immune-informatics study, J. Transl. Med. 17 (1) (2019).